Articles

Electron-Spin Exchange Coupling Transmitted by ^{58,60}Ni ($I = 0$) and ^{59}Co ($I = 7/2$): Does the Nuclear Magnetic Moment of the Spacer Atom Show?[†,1]

Christoph Elschenbroich,* Martin Wünsch, Andreas Behrend, Bernhard Metz, Bernhard Neumüller, and Klaus Harms

Fachbereich Chemie der Philipps-Universität, D-35032 Marburg, Germany

Received May 12, 2005

The trinuclear complexes $\{(Me_2P\text{-}\eta^6\text{-}C_6H_5)_2M\}_2Ni$ **7**$^{\bullet\bullet}$ (M = V), **8** (M = Cr), $\{(Me_2P\text{-}\eta^6\text{-}C_6H_5)_2M\}_2CoH$ **10**$^{\bullet\bullet}$ (M = V), **11** (M = Cr), and $\{(Me_2P\text{-}\eta^6\text{-}C_6H_5)(\eta^6\text{-}C_6H_6)M\}_2Ni(CO)_2$ **14**$^{\bullet\bullet}$ (M = V) and **15** (M = Cr) have been prepared and characterized by means of X-ray crystal structure analysis in two representative cases (**11**, **15**). The "closed" complexes **7**$^{\bullet\bullet}$, **8**, **10**$^{\bullet\bullet}$, and **11** are semirigid, and the "open" species **14** and **15** are conformationally flexible. Magnetocommunication has been studied for the diradicals **7**$^{\bullet\bullet}$, **10**$^{\bullet\bullet}$, **14**$^{\bullet\bullet}$, and **15**$^{\bullet+\bullet+}$ by fluid solution EPR spectroscopy. Comparison of **7**$^{\bullet\bullet}$ with **10**$^{\bullet\bullet}$ shows that the magnetic moment of the nucleus ^{59}Co fails to shape the ^{51}V hyperfine structure in any discernible way. The flexibility of **14**$^{\bullet\bullet}$ furnishes this complex with the largest exchange coupling constant J in the series and is responsible for a pronounced temperature dependence, as demonstrated by alternating EPR line widths upon lowering the temperature. Isoelectronic replacement of V$^{\bullet}$ by Cr$^{\bullet+}$ in the terminal sandwich units yielding **15**$^{\bullet+\bullet+}$ profoundly attenuates the exchange coupling. Cyclic voltammetry reveals that the complex **10**$^{\bullet\bullet}$ engages in a five-step redox chain $2-|-|0|+|2+|3+$. Since the central couple $0|+$ represents the oxidation of the spiro cobalt atom, the redox splitting $\delta E_{1/2}(0|-,-|2-)$ is governed by a neutral spacer and $\delta E_{1/2}(3+|2+,2+|+)$ by a cationic spacer. The positive charge on the spacer exerts a leveling effect in that $\delta E_{1/2}(\text{reduction}) = \delta E_{1/2}(\text{oxidation})$, contrary to spacers of constant charge, for which $\delta E_{1/2}(\text{reduction}) > \delta E_{1/2}(\text{oxidation})$ is commonly observed.

Introduction

Intramolecular communication may be mechanical, as demonstrated by the cooperativity of the four heme groups in hemoglobin,[2] electronic, as exhibited by the mixed/intermediate valence phenomenon,[3] electrochemical, as in the mutual influence multiple redox sites exert on each other's potentials,[4] or magnetochemical, which manifests itself in the effect of electron−electron spin−

spin interaction on EPR and magnetic properties.[5] In all these variants, the intervening medium, commonly called the "spacer", is of utmost importance, and therefore generalizations as to the propagating properties of certain spacer components are in high demand. In this endeavor, because of their well-defined redox and magnetic properties, sandwich complexes serve admirably as probes. The investigation described in the present paper deals with paramagnetic bis(η^6-benzene)-vanadium (**1**$^{\bullet}$) as terminal units in trinuclear complexes and how an intervening complex unit containing Co or Ni as central metal atom influences the interaction

† Dedicated to bis(benzene)chromium on the occasion of its 50th birthday.[20b]

* To whom correspondence should be addressed. E-mail: eb@chemie.uni-marburg.de.

(1) Metal π Complexes of Benzene Derivatives, LVIII. Part LVII: Elschenbroich, Ch.; Pietras, M.; Harms, K. *J. Organomet. Chem.* **2003**, *684*, 359.

(2) Perutz, M. F.; Fermi, G.; Luisi, B.; Shaanan, B.; Liddington, R. C. *Acc. Chem. Res.* **1987**, *20*, 309.

(3) (a) Robin, M. B.; Day, P. *Adv. Inorg. Chem. Radiochem.* **1967**, *10*, 247. (b) Creutz, C. *Prog. Inorg. Chem.* **1983**, *30*, 1. (c) Nelsen, S. F. *Chem. Eur. J.* **2000**, *6*, 581. (d) Demadis, K. D.; Hartshorn, C. M.; Meyer, T. J. *Chem. Rev.* **2001**, *101*, 2655. (e) Ribou, A.-C.; Launay, J.-P.; Sachtleben, M. L.; Li, H.; Spangler, C. W. *Inorg. Chem.* **1996**, *35*, 3735.

(4) (a) Richardson, D. E.; Taube, H. *Inorg. Chem.* **1981**, *20*, 1278. (b) Richardson, D. E.; Taube, H. *Coord. Chem. Rev.* **1984**, *60*, 107. (c) Astruc, D. *Acc. Chem. Res.* **1997**, *30*, 383. (d) Barlow, S.; O'Hare, D. *Chem. Rev.* **1997**, *97*, 637. (e) Ward, M. D.; McCleverty, J. A. *J. Chem. Soc., Dalton Trans.* **2002**, 275.

(5) (a) Paul, F.; Lapinte, C. In *Unusual Structures and Physical Properties in Organometallic Chemistry*; Gielen, M., Willem, R., Wrackmeyer, B., Eds.; Wiley: West Sussex, 2002; pp 219−295. (b) McCleverty, J. A.; Ward, M. D. *Acc. Chem. Res.* **1998**, *31*, 842. (c) Mabbs, F. E. *Chem. Soc. Rev.* **1993**, *22*, 313. Ung, V. A.; Thompson, M. W. C.; Bardwell, A. D.; Gatteschi, D.; Jeffery, J. C.; McCleverty, J. A.; Totti, F.; Ward, M. D. *Inorg. Chem.* **1997**, *36*, 3447. (d) Sutter, J.-P.; Kahn, M. L.; Golhen, S.; Ouahab, L.; Kahn, O. *Chem. Eur. J.* **1998**, *4*, 571. (e) Heinze, K.; Huttner, G.; Schober, P. *Eur. J. Inorg. Chem.* **1998**, 183. (f) Stranger, R.; McGrady, J. E.; Arnold, D. P.; Lane, A.; Heath, G. A. *Inorg. Chem.* **1996**, *35*, 7791. (g) Belanzoni, P., Re, N.; Rosi, M.; Sgamellotti, A.; Baerends, E. J.; Floriani, C. *Inorg. Chem.* **1996**, *35*, 7776. (h) Pardo, E.; Faus, J.; Julve, M.; Lloret, F.; Muñoz, M. C.; Cano, J.; Ottenwaelder, X.; Journaux, Y.; Carrasco, R.; Blay, G.; Fernández, I.; Ruiz-García, R. *J. Am. Chem. Soc.* **2003**, *125*, 10770.

between the terminal units. While being isovalence electronic in the complexes to be studied, the central metals Co ($I = 7/2$) and Ni ($I = 0$) differ in their nuclear magnetic moment. This couple may therefore reveal whether nuclear magnetism of a bridging atom affects the extent of intramolecular communication or manifests itself in the EPR hyperfine pattern which is diagnostic of electron–electron spin–spin exchange coupling in a biradical complex.

Intramolecular magnetocommunication clearly expresses itself in the spin-exchange coupling J of two unpaired electrons that reside on the central metal atoms of two bis(benzene)vanadium units separated by a spacer.[6] We have studied the spacer dependence of the magnitude of J extensively in recent years, employing as a probe (η^7-C_7H_7)V(η^5-C_5H_5), trovacene(**3•**), rather than the symmetrical complex (η^6-C_6H_6)V(η^6-C_6H_6) (**1•**) because the synthesis of derivatives is somewhat more tractable for the former, compared to the latter.[7a] Furthermore, the lower symmetry of trovacene constitutes an additional source of information since the spin densities in the five- and seven-membered rings differ; this governs the intensity of exchange coupling in isomeric dinuclear complexes that are linked via the five- or the seven-membered rings, respectively.[7b] For the synthesis of chelating sandwich complexes, bis(benzene)vanadium is to be preferred, however, because a chelating ligand based on unsymmetrical trovacene can introduce problems caused by isomerism. The work described in this paper deals with the coordination of the "ligands" bis(dimethylphosphano-η^6-benzene)vanadium (**4•**) and bis(dimethylphosphano-η^6-benzene)chromium (**5**) to the spacer atoms ^{58,60}Ni ($I = 0$) and ^{59}Co ($I = 7/2$) (present in the unit Co–H), the question being raised whether the presence of a nuclear spin $I = 7/2$ in the case of cobalt exerts an influence on the magnitude of the exchange coupling constant J. In a physically descriptive sense, spin exchange in a typical biradical, which is defined by a very low value of J, is often rationalized in terms of two concerted intramolecular electron transfer processes whose rate governs the EPR hyperfine pattern. In this picture, the "slow" (weak) exchange limit implies coupling of each individual electron spin to a single nuclear spin only. The magnitude of hyperfine coupling a then is identical to that in a localized monoradical. Conversely, in the "fast" (strong) exchange limit electron spin coupling to the nuclear spins on both sites arises and the ^{51}V hyperfine splitting is halved, causing the hyperfine pattern to mimic that of a delocalized dinuclear monoradical. This visualization gives a feel for the borderline cases and serves to justify the term "exchange" in the name for the parameter J. It also provides a conceptual link between exchange coupling and intramolecular electron and energy transfer. Yet, the more informative EPR hyperfine patterns in the intermediate exchange region call for a more formal treatment invoking singlet–triplet state mixing, which also forms the basis for the spectral simulation routines.[5c,14e]

Adhering to the electron transfer interpretation of exchange coupling, one may pose the question whether, just like in the "chemical mechanism" of inner sphere ET,[8] the electrons "on their way" interact with magnetic nuclei of the bridge, in the present case possibly giving rise to ^{59}Co in addition to ^{51}V hyperfine structure. To test this notion, the organometallic biradicals [(Me$_2$P-η^6-C_6H_5)$_2$V•]$_2$M (**7••**, M = Ni; **10••**, M = CoH) will be described and their EPR spectra compared. Since all three metal centers V, Ni, and Co in the target complexes are redox active, the study of magnetocommunication will be complemented by cyclic voltammetry, which should shed light on electrocommunication present in these trinuclear complexes.

Results and Discussion

Synthesis. Di[bis(dimethylphosphano-η^6-benzene)vanadium]nickel (**7••**) was prepared by lithiation of bis(benzene)vanadium (**1•**) and reaction with dimethylchlorophosphane and then bis(1,5-cyclooctadiene)nickel (**6**). Reaction of bis(dimethylphosphano-η^6-benzene)vanadium (**4•**) with (η^3-cyclooctenyl)(η^4-cycloocta-1,5-diene)cobalt (**9**) yielded di[bis(dimethylphosphano-η^6-benzene)vanadium]cobalt hydride (**10••**) (Scheme 1). The analogous diamagnetic chromium complexes **8**[9] and **11** were prepared accordingly; they formed superior crystals for X-ray crystallography, and their structural features are considered to be representative for the vanadium congeners as well.

While the trinuclear complexes **7••**, **8**,[9] **10••**, and **11** feature a nearly rigid frame, the intermetallic distances being fixed, it was desirable to dispose of complexes with identical coupling paths which are flexible, however. We therefore also prepared the compounds **14••** and **15**, in which the sandwich units are part of monodentate phosphane ligands. In this case, rather than by a spiro nickel center, the ligands are connected by a Ni(CO)$_2$ unit (Scheme 1).

X-ray Crystallography. Drawings of the molecular structures of the complexes **11** and **15** in the crystal are depicted in Figures 1 and 2; pertinent distances and angles are given in the captions. The geometries of the central MP$_4$ cores in the trinuclear complexes **11** and **8**[9] are contrasted in Figure 3. Despite the vicinity of the heavy metal atom cobalt, the hydrogen atom of the Co–H bond could be located; additionally, its presence can be inferred from the structural features of the CoP$_4$ core.[10] The positions of the four P atoms in **11** deviate markedly from tetrahedral in that they are part of a distorted trigonal bipyramid in which the atoms P2, P3, and P4 occupy the equatorial positions and P1 and the hydride ligand reside at the apical position. This de-

(6) (a) Elschenbroich, Ch.; Heck, J. *Angew. Chem., Int. Ed. Engl.* **1981**, *20*, 267. (b) Nowotny, M.; Elschenbroich, Ch.; Behrendt, A.; Massa, W.; Wocadlo, S. *Z. Naturforsch.* **1993**, *48 b*, 1581. (c) Elschenbroich, Ch.; Metz, B.; Neumüller, B.; Reijerse, E. *Organometallics* **1994**, *13*, 5072. (d) Elschenbroich, Ch.; Bretschneider-Hurley, A.; Hurley, J.; Behrendt, A.; Massa, W.; Wocadlo, S.; Reijerse, E. *Inorg. Chem.* **1995**, *34*, 743.

(7) (a) Elschenbroich, C.; Schiemann, O.; Burghaus, O.; Harms, K. *Chem. Commun.* **2005**, 2149, and previous papers in the series "Trovacene Chemistry". (b) Elschenbroich, Ch.; Plackmeyer, J.; Harms, K.; Burghaus, O.; Pebler, J. *Organometallics* **2003**, *22*, 3367.

(8) (a) Wilkins, R. G. *Kinetics and Mechanism of Reactions of Transition Metal Complexes,* 2nd ed.; VCH: Weinheim, 1991; Chapter 5.8. (b) Jordan, R. B. *Reaction Mechanisms of Inorganic and Organometallic Systems,* 2nd ed.; Oxford University Press: New York, 1998; Chapter 6.4. (c) Beitz, J. V.; Miller, J. R.; Cohen, H.; Wieghardt, K.; Meyerstein, D. *Inorg. Chem.* **1980**, *19*, 966.

(9) Elschenbroich, Ch.; Heikenfeld, G.; Wünsch, M.; Massa, W.; Baum, G. *Angew. Chem., Int. Ed. Engl.* **1988**, *27*, 414.

(10) (a) Frentz, B. A.; Ibers, J. A. *Inorg. Chem.* **1970**, *11*, 2403. (b) Holah, D. G.; Hughes, A. N.; Maciaszek, S.; Magnuson, V. R.; Parker, K. O. *Inorg. Chem.* **1985**, *24*, 3956.

Scheme 1
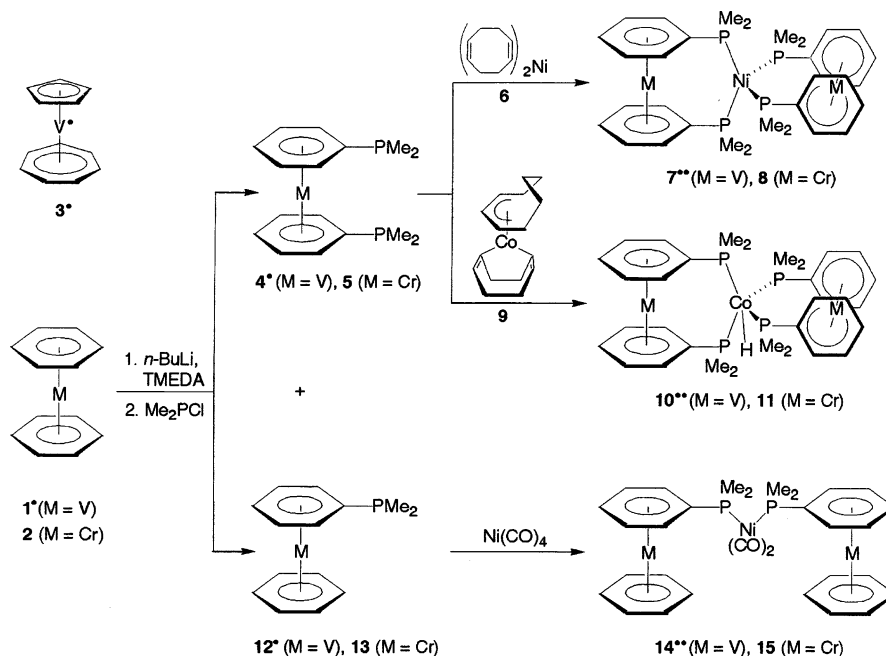
scription is supported by the fact that the cobalt atom lies only 40 pm from the plane defined by P2, P3, and P4, whereas in tetrahedral coordination this distance would amount to 70 pm assuming identical Co–P bond lengths. Furthermore, the angles P2CoP3 (123°) and P2CoP4 (120°) also point to a flattening of the internal trigonal pyramid P2P3P4Co since these angles should amount to 109.5° if Co resided at the center of a tetrahedron P1P2P3P4. Conversely, the angles P1CoP2 (97°), P1CoP3 (100°), and P1CoP4 (106°) are smaller than that encountered in an undistorted tetrahedron. The intermetallic distance of the terminal chromium atoms is affected only marginally, though, by hydride–ligand-induced distortion in that $d(\mathrm{Cr}\cdots\mathrm{Cr}) = 849.0$ (**8**),

861.5 pm (**11**), this difference partially being attributable to the larger covalent radius of Co, compared to Ni.

In the structure of the "open" congener **15**, as expected, the interchromium distance $d(\mathrm{Cr}\cdots\mathrm{Cr}) = 947$ pm exceeds that found for the "closed" trinuclear complexes **8** and **11**. Of course, this gradation of intermetallic distances is not transferable to fluid solution, where the extent of intramolecular communication was studied by means of EPR spectroscopy and cyclic voltammetry. The dimensions of the bis(arene)metal units are affected insignificantly by their incorporation into the trinuclear complexes **8**, **11**, and **15**.

NMR Spectroscopy. The most significant ¹H NMR feature of complex **11** is the resonance at δ −12.92, which appears as a quintet, $J(^{1}\mathrm{H},^{31}\mathrm{P}) = 32$ Hz, and can
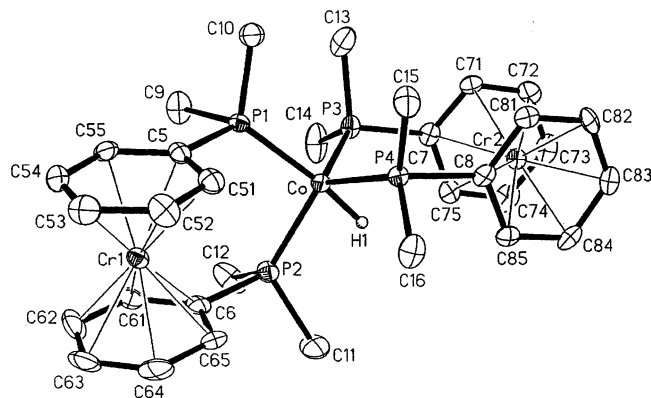

Figure 1. Molecular structure of di[bis(dimethylphosphano-η^6-benzene)chromium]cobalt hydride (**11**), ORTEP plot (50% probability ellipsoids). Selected bond lengths (Å) and bond angles (deg): Co–P1 2.146(2), Co–P2 2.132(2), Co–P3 2.136(2), Co–P4 2.138(1), P1–C5 1.843(5), P2–C6 1.846(5), P3–C7 1.836(5), P4–C8 1.860(5), P1–Co–P2 96.81(6), P1–Co–P3 100.00(6), P1–Co–P4 106.28(6), P2–Co–P3 122.54(6), P3–Co–P4 106.97(6), P2–Co–P4 120.03-(6), sandwich tilt angles 1.0 (Cr1), 2.0 (Cr2), intersandwich angle 80.5, Cr1···Co 4.472(1), Cr2···Co 4.343(1), Cr1···Cr2 8.615(1).
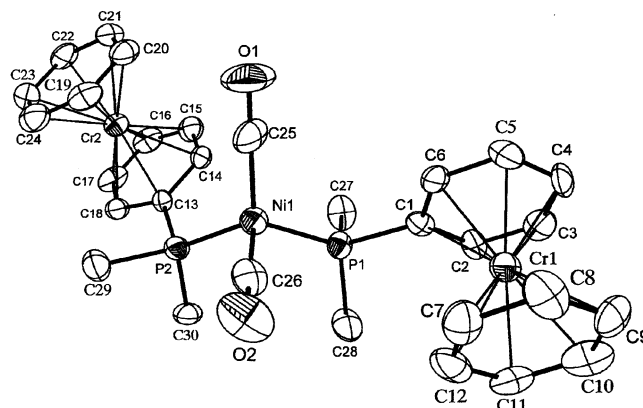
Figure 2. Molecular structure of di[bis(dimethylphosphano-η^6-benzene)chromium]nickel (**15**), ORTEP plot (50% probability ellipsoids). Selected bond lengths (Å) and bond angles (deg): Ni1–P1 2.207(2), Ni1–P2 2.217(2), Ni1–C25 1.747(6), Ni1–C26 1.786(7), P1–C1 1.813(8), P2–C13 1.813(7), C25–O1 1.155(7), C26–O2 1.122(8), P1–N1–C25 111.9(3), P2–Ni1–C25 110.5(3), C25–Ni1–C26 114.2(3), P1–Ni1–C26 107.0(3), P2–Ni1–C26 107.0(2), P1–Ni1–P2 105.8(3), Cr1···Ni1 4.9089(16), Cr2···Ni1 4.9006(16), Cr1···Cr2 9.478(2).
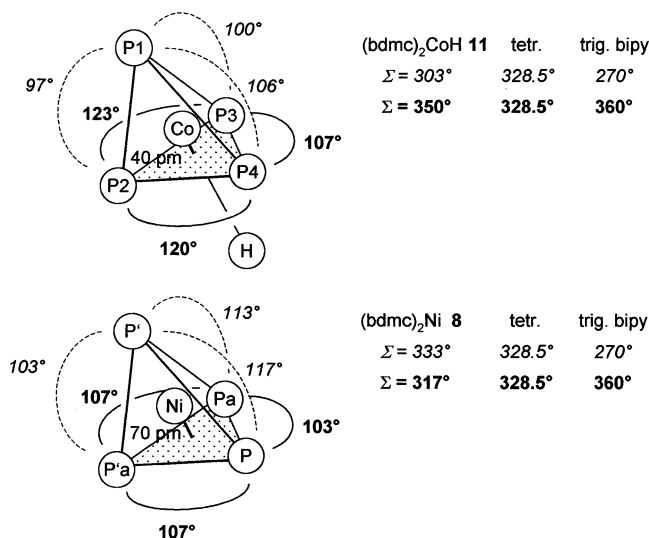
Figure 3. Bond angles $P(i)MP(j)$ in the central MP_4 cores of the trinuclear complexes 8[9] and 11. Note that in 8 the sums of angles $\Sigma(<)$ and $\Sigma(\cdot\because)$ approach those expected for tetrahedral coordination of Ni, whereas for 11 they signal distortion toward trigonal bipyramidal coordination.

be assigned to the metal-bonded hydrogen atom. The absence of discernible splitting caused by scalar coupling $J(^1H,{}^{59}Co)$ must be traced to the short relaxation time effected by the large quadrupole moment of the nucleus ^{59}Co. $^{31}P\{^1H\}$ NMR of 11 exhibits a single resonance at δ 11.8, which, together with the quintet structure of the proton signal of the P_4Co-H segment, signalizes apparition of a dynamic process. Reversion of three-membered interannular bridges at sandwich complexes is a well-known phenomenon, which has been observed in the ferrocene[11a,b] as well as in the bis(arene)metal[11c,d] series. Apart from the equivalence of the P atoms, cycloreversion is also responsible for that of the methyl groups, which in the frozen configuration, present in the crystal, adopt axial and equatorial positions. Strictly speaking, the complexes $7^{\bullet\bullet}$, 8, $10^{\bullet\bullet}$, and 11 should be designated as "semirigid", thereby implying that some conformational mobility is encountered, which, however, does not grossly change the mutual disposition of the terminal metal atoms that engage in intramolecular communication. This contrasts with the singly bridged complexes $14^{\bullet\bullet}$ and 15, which possess more degrees of conformational freedom with attendant variability of intermetallic distances and extent of communication.

EPR Spectroscopy. Oligoradical complexes based on bis(η^6-benzene)vanadium(d^5) ($1^{\bullet}$) or its unsymmetrical isomer (η^7-tropylium)vanadium(d^5)(η^5-cyclopentadienyl), trovacene ($3^{\bullet}$), as paramagnetic probes give rise to ^{51}V hyperfine patterns from which the magnitude of the exchange coupling constant J can be extracted if the latter falls in the range $5 \times 10^{-4} \lesssim |J| \lesssim 1.5$ cm^{-1} or 0.1 $a(^{51}V) \lesssim |J| \lesssim 300\ a(^{51}V)$.[5c,12] In this regime the EPR spectra significantly deviate from the borderline cases

(11) (a) Davison, A.; Smart, J. C. *J. Organomet. Chem.* **1979**, *174*, 321. (b) Abel, E. W.; Long, N. J.; Orrell, K. G.; Osborne, A. G.; Sik, V.; Bates, P. A.; Hursthouse, M. B. *J. Organomet. Chem.* **1989**, *367*, 275. (c) Benn, R.; Blank, N. E.; Haenel, M. W.; Klein, J.; Koray, A. R.; Weidenhammer, K.; Ziegler, M. L. *Angew. Chem., Int. Ed. Engl.* **1980**, *19*, 44. (d) Elschenbroich, Ch.; Burdorf, H.; Mahrwald, D.; Metz, B. *Z. Naturforsch.* **1992**, *47b*, 1157.
(12) Elschenbroich, Ch.; Plackmeyer, J.; Nowotny, M.; Behrendt, A.; Harms, K.; Pebler, J.; Burghaus, O. *Chem. Eur. J.* **2005**, in press.
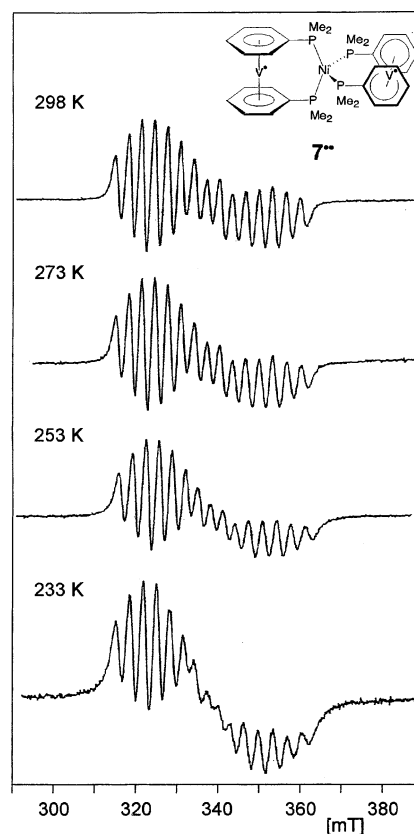

Figure 4. EPR spectrum (X-band) of di[bis(dimethylphosphano-η^6-benzene)vanadium]nickel ($7^{\bullet\bullet}$), toluene, 298 K, g = 1.988, $|J|$ = 0.29 cm^{-1}; temperature dependence of the ^{51}V hyperfine pattern.
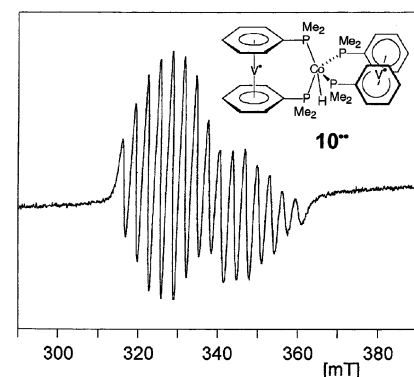

Figure 5. EPR spectrum (X-band) of di[bis(dimethylphosphano-η^6-benzene)vanadium]cobalt hydride ($10^{\bullet\bullet}$), toluene, 298 K, g = 1.987, $|J|$ = 0.33 cm^{-1}.

of an octet of lines of equal intensity spaced by $a(^{51}V)$ and a quindecet of relative intensities 1:2:3:4:5:6:7:8:7: 6:5:4:3:2:1, spaced by $a(^{51}V)/2$. The EPR spectra of $7^{\bullet\bullet}$ (Figure 4), $10^{\bullet\bullet}$ (Figure 5), and $14^{\bullet\bullet}$ (Figure 6) clearly reflect situations between these limiting cases and therefore are amenable to interpretation and computer simulation (Figure 7). In this way the exchange coupling constants $|J(7^{\bullet\bullet})|$ = 0.29, $|J(10^{\bullet\bullet})|$ = 0.33, and $|J(14^{\bullet\bullet})|$ = 0.42 cm^{-1} are determined for the spectra recorded at 298 K. Most importantly, hyperfine coupling to ^{59}Co is absent in the spectrum of $10^{\bullet\bullet}$ and the ability of the units P_4Ni and P_4CoH to promote exchange coupling is very similar; the slightly larger value of $J(10^{\bullet\bullet})$ compared to $J(7^{\bullet\bullet})$ may be traced to the larger atomic radius and higher electron density on Co^{-I} compared to Ni^0.
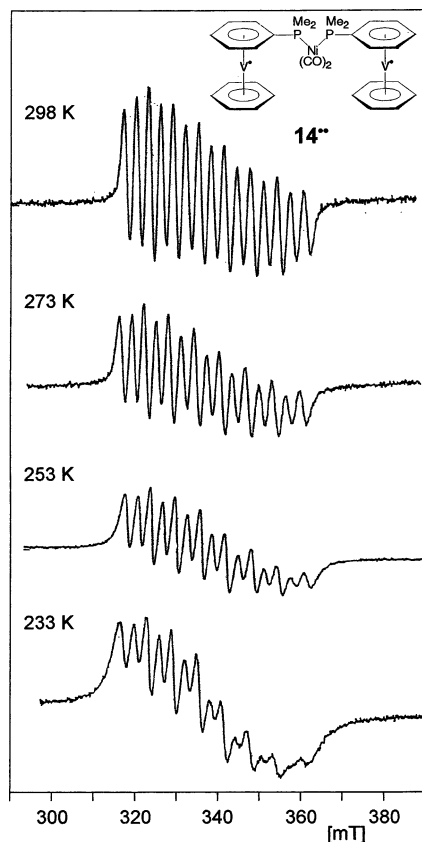
Figure 6. EPR spectrum (X-band) of di[(η^6-benzene)-(dimethylphosphano-η^6-benzene)vanadium]di(carbonyl)-nickel (**14$^{\bullet\bullet}$**), toluene, 298 K, g = 1.9843, $|J|$ = 0.42 cm^{-1}; temperature dependence of the ^{51}V hyperfine pattern.
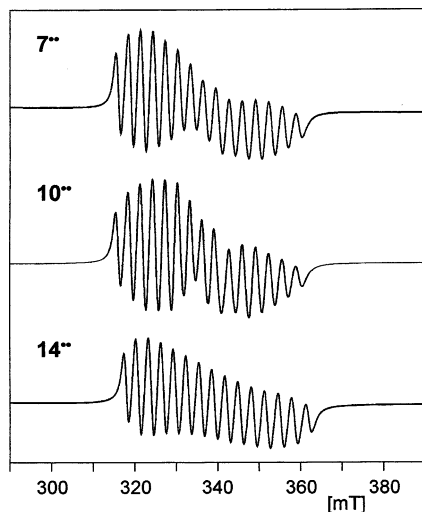
Figure 7. Simulations[14e] of the EPR spectra (298 K) of the organometallic biradical species **7$^{\bullet\bullet}$** ($|J|$ = 0.29 cm^{-1}, Figure 4), **10$^{\bullet\bullet}$** ($|J|$ = 0.33 cm^{-1}, Figure 5), and **14$^{\bullet\bullet}$** ($|J|$ = 0.42 cm^{-1}, Figure 6).

A drastic weakening of the exchange interaction is observed if in the neutral diradical **7$^{\bullet\bullet}$** in the terminal sandwich units V^0 is replaced by Cr$^{\bullet+}$ to yield the isoelectronic diradical dication **8$^{\bullet+\bullet+}$**. This species has been studied previously, and the most important result, within the context of this discussion, was the detection of ^{1}H and ^{53}Cr hyperfine structure caused by $a(1^{53}$Cr) = 17.7 G and $a(10^1$H) = 3.23 G.[9] Theses parameters mimic those of the mononuclear species **5$^{\bullet+}$**, thereby
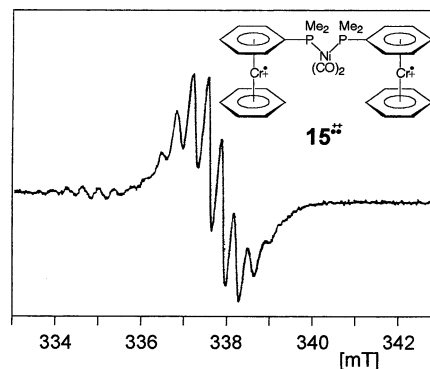

Figure 8. EPR spectrum (X-band) of the di[(η^6-benzene)-(dimethylphosphano-η^6-benzene)chromium(I)]di(carbonyl)-nickel dication (**15$^{\bullet+\bullet+}$**), DMF/CHCl$_3$ (1:1), 298 K, g = 1.9859, $a(11\ ^1$H) = 0.341 mT, $a(1\ ^{53}$Cr) = 1.83 mT. High-field ^{53}Cr satellites broadened beyond recognition due to large molecular size and small tumbling rate.

implying that $J(\mathbf{8^{\bullet+\bullet+}}) \ll a(^1$H, $\mathbf{8^{\bullet+\bullet+}}$), $a(^{53}$Cr, $\mathbf{8^{\bullet+\bullet+}}$). Conversely, EPR had revealed that, despite the gradation $a(^{51}$V, $\mathbf{7^{\bullet\bullet}}) > a(^{53}$Cr, $\mathbf{8^{\bullet+\bullet+}}$), $a(^1$H, $\mathbf{8^{\bullet+\bullet+}}$) for the neutral diradical $J(\mathbf{7^{\bullet\bullet}}) > a(^{51}$V, $\mathbf{7^{\bullet\bullet}}$) holds. Therefore, the two isoelectronic species exhibit strongly differing extents of exchange coupling in that $J(\mathbf{7^{\bullet\bullet}}) \gg J(\mathbf{8^{\bullet+\bullet+}})$. Irrespective of the intimate coupling mechanism, this finding can be rationalized by the contracted nature of the singly occupied metal orbital in a cation compared to a neutral species. For the same reason $J(\mathbf{14^{\bullet\bullet}})$ (Figure 6) implies intermediate exchange and $J(\mathbf{15^{\bullet+\bullet+}})$ (Figure 8) weak exchange coupling on the hyperfine time scale.

The relation $J(\mathbf{14^{\bullet\bullet}}) > J(\mathbf{10^{\bullet\bullet}})$ may initially come as a surprise since, rather than two as in **10$^{\bullet\bullet}$**, only one link PNiP connects the two paramagnetic sandwich units in **14$^{\bullet\bullet}$**. However, the high conformational flexibility of "open" **14$^{\bullet\bullet}$** must be invoked, which enables the molecule to adopt momentary structures favorable for exchange coupling, including the case of collisional encounter of the two paramagnetic sandwich units with the effect that direct exchange (through-space) can add to or compete with superexchange (through bond).

Conformational rigidity of **7$^{\bullet\bullet}$** versus flexibility of **14$^{\bullet\bullet}$** serves to explain the disparate response of the EPR spectra to temperature change (Figures 4 and 6). While the spectrum of **7$^{\bullet\bullet}$** apart from slight general line broadening is essentially unaffected, the spectrum of **14$^{\bullet\bullet}$** changes significantly in increasingly reverting to an alternating line widths pattern as the temperature is lowered; the effect expresses itself more clearly in alternating amplitudes of consecutive lines. Superimposed on this pattern is the familiar low-|center-|high field line widths variation which results from tumbling motion insufficient to average g and hyperfine anisotropies.[13] Alternating line widths in exchange coupled EPR spectra are caused by fluctuations of the coupling constant J about its static value, which accompanies intramolecular conformational changes.[14] They were first observed for bisnitroxides[14a,b] and later for dinuclear paramagnetic transition metal complexes,[14d] no example having been found for organometallic species yet as far as we know. In the present case **14$^{\bullet\bullet}$** modula-

(13) (a) Wilson, R.; Kivelson, D. *J. Chem. Phys.* **1966**, *44*, 154. (b) Atkins, P. W.; Kivelson, D. *J. Chem. Phys.* **1966**, *44*, 169. (c) Chasteen, N. D.; Hanna, M. W. *J. Phys. Chem.* **1972**, *76*, 3951.
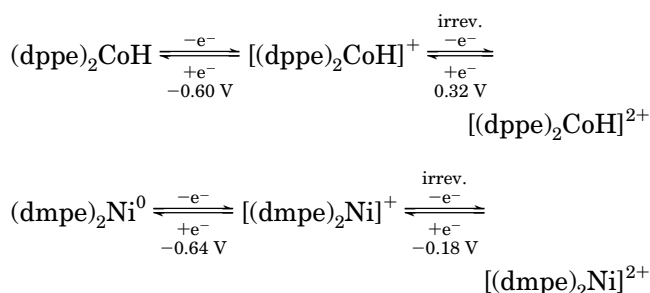
Scheme 2

16 (M = V)
17 (M = Cr$^+$)

18
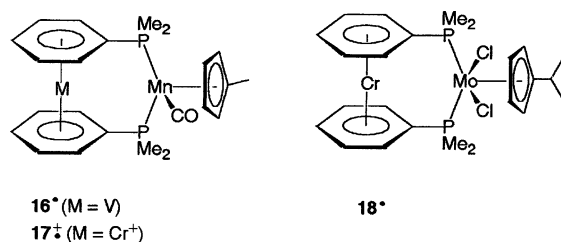
tion of J is effected by time-dependent changes of the intervanadium distance. From the aforesaid it is clear that a large number of parameters would enter into spectral simulation because the influence of tumbling motion as well as that of conformational change on the line widths must be included. The requisite expressions are given in a paper by Mabbs.[14d] This paper also features the EPR spectrum of an acetylene dicarboxylic acid-bridged oxovanadium(IV) dimer that strongly resembles that of the organometallic biradical **14""**; the interpretations should be closely related in both cases. Accordingly, the simulations in the present work have been performed with a program based on the Mabbs approach.[14e]

Returning to the initial question whether a magnetic nucleus as part of a bridge that mediates exchange coupling gives rise to EPR hyperfine structure, the absence of discernible ^{59}Co splitting in the spectrum of **10""** should be commented on. Isotropic hyperfine interaction requires finite s orbital spin density at the magnetic nucleus. In paramagnetic transition metal complexes this usually arises from spin polarization of inner s shells, brought about by partially occupied d orbitals of the central metal atom. Bis(arene)metal complexes that bear a metal atom with a magnetic moment in an interannular link have been studied previously with the aim of assessing interaction between the two types of metal atoms present (Scheme 2). Whereas the EPR spectrum of complex **16"** reveals ^{51}V hyperfine structure only, no indications for ^{55}Mn splitting being detectable, from the spectrum of the isoelectronic cation **17"+** the value $a(^{55}\mathrm{Mn}) = 0.8$ G can be extracted.[15a] The lack of resolution of ^{55}Mn hyperfine splitting in the case of **16"** is probably caused by the larger intrinsic line width for **1"** ($\approx$5 G) compared to **2"+** ($\approx$0.5 G), under which spectral detail may be hidden. No a priori decision as to the mechanism of spin transfer to the nucleus ^{55}Mn in **17"+** can be offered; both a direct mechanism (through-space) and a superexchange path (through-bond) can operate, although the large distance $d(\mathrm{Cr}\cdots\mathrm{Mn}) = 453$ pm disfavors the former. In a similar vein, no ^{53}Cr satellites in addition to ^{95,97}Mo satellites are seen in the EPR spectrum of **18"**; intermetallic interaction reveals itself in the rigid solution spectrum

of the diradical cation **18""+**, however, as zero-field splitting and the observation of a $\Delta M_s = 2$ signal.[15b] These observations agree with the habit of the spectrum of **10""** in that the small magnitude of the coupling constant $a(^{59}\mathrm{Co})$ fails to cause discernible splitting of each of the ^{51}V components. The small exchange coupling constant $J(\mathbf{10""})$ and the distribution of total intensity over 15 lines render the $\Delta M_s = 2$ transition too weak for observation (fluid solution), and the large interspin distance of 860 pm in the point dipole approximation gives rise to a zero-field splitting parameter D that is too small to shape the rigid solution spectrum.

Although the presence of magnetic ^{59}Co in the spacer is not obvious from the EPR spectrum of **10""**, it is tempting to speculate about the nature of exchange coupling operative in the diradicals **7""**, **8"+"+**, **10""**, and **11"+"+**. The information from the EPR spectrum of **16"** that finite spin density is transferred from vanadium (d^5) to manganese (low-spin d^6) and the fact that in the trinuclear diradicals Mn is replaced by Ni (**7""**, **8"+"+**) or Co–H (**10""**, **11"+"+**) in a spiro disposition suggest that two orthogonal orbitals at the connecting central metal atom are polarized in a parallel fashion. The P$_4$M linker in these diradicals should therefore mediate weak ferromagnetic coupling, albeit of minute size, given the small spin density transferred to the linker metal atom, as demonstrated by the small hfc constant $a(^{55}\mathrm{Mn})$ in **16"+**.

Electrochemistry. The complexes **7""**, **8**, **10""**, **11**, **14""**, and **15** contain three redox-active metal atoms, which occur as a pair in the terminal sandwich units and a single atom in the spacer. Whereas the presence or absence of a magnetic moment of course is immaterial for the redox properties, it is worthwhile to search for electrocommunication in these species because the variation of charge of a spacer is a novel feature. The results of an examination of the complexes **7""**, **8**, **10""**, and **11** by cyclic voltammetry are collected in Table 1. Assignment of the waves is assisted by reference to the redox properties of the parent complexes **1"** and **2**[16] and of mononuclear complexes that are representative for the spacers:[17]

$$(\mathrm{dppe})_2\mathrm{CoH} \underset{\substack{+e^- \\ -0.60\,\mathrm{V}}}{\overset{-e^-}{\rightleftharpoons}} [(\mathrm{dppe})_2\mathrm{CoH}]^+ \underset{\substack{+e^- \\ 0.32\,\mathrm{V}}}{\overset{\substack{\mathrm{irrev.} \\ -e^-}}{\rightleftharpoons}}$$

$$[(\mathrm{dppe})_2\mathrm{CoH}]^{2+}$$

$$(\mathrm{dmpe})_2\mathrm{Ni}^0 \underset{\substack{+e^- \\ -0.64\,\mathrm{V}}}{\overset{-e^-}{\rightleftharpoons}} [(\mathrm{dmpe})_2\mathrm{Ni}]^+ \underset{\substack{+e^- \\ -0.18\,\mathrm{V}}}{\overset{\substack{\mathrm{irrev.} \\ -e^-}}{\rightleftharpoons}}$$

$$[(\mathrm{dmpe})_2\mathrm{Ni}]^{2+}$$

The most complete picture is drawn by complex **10""** in that five reversible waves spread over a potential range of 2.5 V are observed (Figure 9). The central wave at -0.91 V represents the Co$^{+/2+}$ couple of the P$_4$CoH link; the cathodic shift of -0.31 V relative to the

(14) (a) Luckhurst, G. R. *Mol. Phys.* **1966**, *10*, 543. (b) Glarum, H. S.; Marshall, J. H. *J. Chem. Phys.* **1967**, *47*, 1374. (c) Hudson, A.; Luckhurst, G. R. *Chem. Rev.* **1969**, *69*, 191. (d) Collison, D.; Mabbs, F. E.; Turner, S. S. *J. Chem. Soc., Faraday Trans.* **1993**, *89*, 3705. (e) Burghaus, O. EPR fitting and simulation program "SIMEPR"; University of Marburg, available on request; Burghaus, O. *Proceedings of the Joint 29th AMPERE–13th ISMAR International Conference*; Technische Universität Berlin, 1998; *Magnetic Resonance and Related Phenomena*, Vol. II, p 1186. See also ref 5c.

(15) (a) Elschenbroich, Ch.; Isenburg, T.; Metz, B.; Behrendt, A.; Harms, K. *J. Organomet. Chem.* **1994**, *481*, 153. (b) Elschenbroich, Ch.; Isenburg, T.; Behrendt, A. *Inorg. Chem.* **1995**, *34*, 6565.

(16) Elschenbroich, Ch.; Bilger, E.; Metz, B. *Organometallics* **1991**, *10*, 2823.

(17) The redox properties of these reference molecules have been redetermined in the medium dimethoxyethane/(n-Bu)$_4$NClO$_4$. Different behavior has been reported for the more strongly solvating medium toluene/acetonitrile (1:1): Pilloni, G.; Schiavon, G.; Zotti, G.; Zecchin, S. *J. Organomet. Chem.* **1977**, *134*, 305.

Table 1. Cyclovoltammetric Data for the Trinuclear Complexes 7··, 8, 10··, and 11[a]

[V]	7··	8[b]	10··	11
$E_{1/2}$ (3+|2+)	−0.05	−0.52	−0.08	∼−0.48[g]
ΔE_p	0.115	0.065	0.061	∼0.08
r^c	0.5[d]	1	1	1
$E_{1/2}$(2+|+)	−0.18	−0.70[e]	0.20	∼−0.58[g]
ΔE_p	0.115	0.065	0.088	∼0.08
r^c	1	1	1	1
$E_{1/2}$(+|0)	−0.59	−0.70[e]	−0.91	−0.85
ΔE_p	0.112	0.065	0.055	0.086
r^c	1	1	1	1
$E_{1/2}$(0|−)	−2.66		−2.24	
ΔE_p	0.074		0.055	
r^c	∼1		1	
$E_{1/2}$(−|2−)	−2.80[f]		−2.36	
ΔE_p			0.085	
r			1	

[a] DME/(n-Bu)$_4$ClO$_4$, 221 K (7··, 10··), 293 K (8, 11), 100 mV/s at glassy carbon vs SCE, $E_{1/2} = (E_{pa} + E_{pc})/2$, $\Delta E_p = E_{pa} − E_{pc}$, $r = I_{pa}/I_{pc}$. [b] Additional wave $E_{pa} = −0.12$ V (irrev, 293 K), −0.16 V (rev, 248 K), ref 9. [c] The r values are estimates because in the majority of cases overlapping, partially resolved waves are obtained. [d] Dependent on scan rate. [e] $n = 2$ (electrons transferred). [f] E_{pc}, irrev process. [g] Barely resolved.
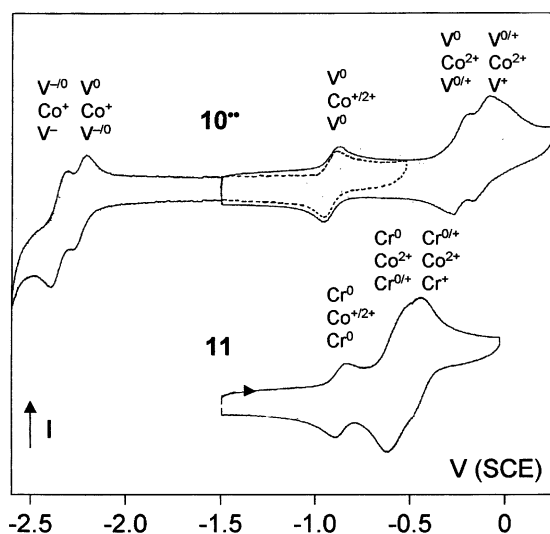

Figure 9. Cyclovoltammetric traces for {(Me$_2$P-η^6-C$_6$H$_5$)$_2$V}$_2$CoH (10··) and {(Me$_2$P-η^6-C$_6$H$_5$)$_2$Cr}$_2$CoH (11), DME, 0.1 M (n-Bu)$_4$NClO$_4$, 221 K, and assignment of the redox sites. Reduction of the chromium atoms in 11 is beyond the cathodic border of the medium.

reference complex (dppe)$_2$CoH reflects the well-known electron-donating character of bis(arene)metal(0) units. The central wave is flanked by two clearly resolved pairs of waves that indicate vanadium-centered consecutive reductions and oxidations, respectively, showing redox splittings $\delta E_{1/2}$ of 120 mV. This is remarkable since interaction occurs across a seven-bond separation, including orbital orthogonality at the central spiro junction. It comes as a surprise, however, that the redox splitting $\delta E_{1/2}$ of the two peripheral reductions and oxidations for 10·· are of equal magnitude because in all previous cases the $\delta E_{1/2}$(2+|+,+|0) values were considerably smaller (≈$^2/_3$) than those for the $\delta E_{1/2}$-(0|−,−|2−) pair.[7b] A novel aspect in the present work is the fact that the reductions are mediated by a Co$^+$-containing spacer, whereas oxidations experience a Co^{2+} spacer. The observation that the higher positive charge on the spacer serves to equalize the $\delta E_{1/2}$(reductions)

and $\delta E_{1/2}$(oxidations) parameters is discomforting in view of previous interpretations, which had traced the gradation $\delta E_{1/2}$(reductions) > $\delta E_{1/2}$(oxidations) to metal orbital contraction with attendant attenuation of metal−ligand interaction.[7b] Why, then, is the Co^{2+} spacer a more efficient mediator of electrocommunication than the Co$^+$ spacer?

If the peripheral sandwich units contain chromium instead of vanadium as the central metal atom (11), only oxidations are registered since reduction would entail generation of a 19 VE configuration, which, because of the extremely negative requisite potential, is way beyond the electrochemical window. The chain of oxidation steps is again started with the Co$^{+/2+}$ couple, followed by barely resolved oxidations Cr$^{0/+}$ within the terminal sandwich units. A very similar sequence of redox steps arises if CoH in the spacer is substituted by Ni. As for CoH in the complexes 10·· and 11, primary oxidation of the spiro-Ni atom in 7·· occurs at a more negative potential, compared to the reference molecule (dmpe)$_2$Ni. Establishment of a positive charge on the spiro-Ni$^+$ ion then causes anodic shifts of the subsequent V$^{0/+}$ oxidations, compared to parent 1·, and they exhibit a redox splitting $\delta E_{1/2}$ of 130 mV. This value, which has been encountered repeatedly in the series under investigation, appears to be characteristic for a tetrahedral P$_4$M spacer unit, irrespective of the nature of M and of that of the interacting peripheral metal atoms. While this invariance could trivially be rationalized under the assumption of through-space electrostatic interactions between the redox sites, the large intermetal distance of 860 pm renders this approach unrealistic and an alternative through-bond mechanism of electrocommunication should be searched for. This is devised easily since primary metal-centered oxidation of one sandwich unit will decrease the donor and increase the acceptor character of this metal with attendant change of the donor/acceptor ratio of η^6-arylphosphane with regard to the spacer metal atom. Propagation of this effect across the molecule will ultimately lower the electron density on the second peripheral metal atom, thereby causing an anodic shift of the potential $E_{1/2}$(M$^{0/+}$).

By way of conclusion and in response to the quest of this paper it can be stated that the magnetic moment of the nucleus ^{59}Co, which is part of the spacer in the trinuclear complex 10··, is unnoticed in that neither the magnitude of exchange coupling J of the peripheral paramagnetic bis(benzene)vanadium units is affected nor does the hyperfine pattern show resolved ^{59}Co splitting. In fact, the EPR spectra of the ^{59}Co ($I = ^7/_2$)- and ^{58,60}Ni ($I = 0$)-containing species are almost identical. Access to the oxidation states Co$^+$ and Co^{2+} in 10·· permits a study of the influence of a change of charge in the spacer on the extent of electrocommunication. It is found that a positive charge in the spacer exerts a leveling effect on the redox splittings $\delta E_{1/2}$(10·· 0|−,−|2−) and $\delta E_{1/2}$(10·· 3+|2+,2+|+) in that both values are equal. This contrasts with the usual observation in cases where the spacer is uncharged that $\delta E_{1/2}$(reductions) exceeds $\delta E_{1/2}$(oxidations) by ≈50%, a disparity that remains to be explained.

Experimental Section

Methods and Materials. All manipulations were performed with exclusion of air under dinitrogen or argon (CV)

Table 2. Crystallographic Data for 11 and 15

	11	15
instrument	P3 (Siemens)	P4 (Siemens)
radiation	Mo Kα	Mo Kα
formula	$C_{32}H_{45}Cr_2CoP_4$	$C_{30}H_{34}Cr_2NiO_2P_2$
fw	716.53	651.22
cryst size (mm)	$0.6 \times 0.4 \times 0.08$	$0.4 \times 0.3 \times 0.2$
a (Å)	17.426(5)	10.180(1)
b (Å)	10.120(3)	11.369(1)
c (Å)	18.737(6)	14.333(2)
α (deg)	90	111.64(1)
β (deg)	108.34(2)	100.24(1)
γ (deg)	90	103.59(1)
V (Å³)	3137(2)	1433.1(3)
cryst syst	monoclinic	triclinic
space group	$P2_1/c$	$P\bar{1}$
no.[25]	14	2
Z	4	2
ρ_{calcd} (g/cm³)	1.517	1.509
temp (K)	203	223
μ (cm⁻¹)	14.3	15.32
$2\theta_{max}$ (deg)	50.00	55.00
h, k, l values	$-20 \le h \le 19$	$-1 \le h \le 12$
	$0 \le k \le 2$	$-1 \le k \le 13$
	$0 \le l \le 22$	$-18 \le l \le 17$
no. of reflns	6054	3690
no. of unique reflns (R_{int})	5511 (0.0503)	3544 (0.0125)
no. of reflns with $F_o > 4\sigma(F_o)$	3423	2180
no. of params	356	338
$R_1{}^a$	0.0451	0.0447
wR_2 (all data)^b	0.1094^c	0.1112^d
max/min resid electron density (e/Å³)	0.86/−0.60	0.46/−0.66

$^a \sum||F_o| - |F_c||/\sum|F_c|.$ $^b wR_2 = \{[w(F_o^2 - F_c^2)^2]/[w(F_o^2)^2]\}^{1/2}.$ $^c w = 1/[\sigma^2(F_o^2) + (0.0553P)^2]; P = [\max(F_o^2, 0) + 2F_c^2]/3.$ $^d w = 1/[\sigma^2(F_o^2) + (0.0662)^2].$

employing standard Schlenk techniques. Bis(η^6-benzene)-vanadium (1·),[20a] bis(η^6-benzene)chromium (2),[20b] (Me$_2$P-η^6-C$_6$H$_5$)(η^6-C$_6$H$_6$)Cr (13),[9] (Me$_2$P-η^6-C$_6$H$_5$)$_2$Cr (5),[9] {(Me$_2$P-η^6-C$_6$H$_5$)$_2$Cr}$_2$Ni (8),[9] and (η^3-cyclooctenyl)(η^4-1,5-cyclooctadiene)cobalt (9)[19] were prepared as described in the literature. All other chemicals were commercially available and were used as received.

Physical measurements were carried out with the following instruments: mass spectrometry, CH 7 (EI-MS), Varian MAT; cyclic voltammetry, potentiostat 552, function generator 568, multipurpose unit 563 Amel, glassy carbon working electrode, SCE reference electrode, Pt auxiliary electrode, solvent/electrolyte DME/10⁻³ M (n-Bu)$_4$NClO$_4$, −35 °C, argon protection; EPR spectroscopy, ESP 300 (X-band), Bruker, frequency counter TR 5214, Advantest.

X-ray Structure Determination of 11 and 15. The crystals were covered with a perfluorinated polyether and mounted at the top of a glass capillary under a flow of cold gaseous nitrogen. The measured intensities were corrected for Lorentz and polarization effects and by a numerical absorption correction (cell parameters, instruments, and radiation see Table 2). The structures were solved by direct methods (SHELXS-86[21]). Refinement was performed against F^2 by full-

matrix least squares with the programs SHELXL-93[22] (11) and SHELXL-97[23] (15). The positions of the H atoms in 11 and 15 were calculated for ideal positions. A common displacement parameter was refined in 11. The calculation of the bond lengths, bond angles, and U_{eq} for 11 was performed with the program PLATON.[24] Crystallographic data for the structures reported in this paper have been deposited with the Cambridge Crystallographic Data Centre as Supplementary Publications Nos. CCDC 280180 (11) and CCDC 270617 (15). These data can be obtained free of charge via www.ccdc.cam.ac.uk/datarequest/cif.

(Me$_2$P-η^6-C$_6$H$_5$)$_2$V (4·) and (Me$_2$P-η^6-C$_6$H$_5$)(η^6-C$_6$H$_6$)V (12·). Bis(benzene)vanadium (1·) (1.34 g, 6.5 mmol) in 120 mL of cyclohexane is reacted at 80 °C during 2 h with n-butyllithium (1.6 M in hexane, 9.3 mL, 14.9 mmol) and N,N,N′,N′-tetramethylethylenediamine, TMEDA (2.2 mL, 14.9 mmol), whereby a reddish brown precipitate of lithiated 1· forms. After cooling to room temperature a solution of dimethylchlorophosphane (4.0 mL, 14.9 mmol) in 20 mL of cyclohexane is added during 30 min under vigorous stirring. Reaction is allowed to proceed for 24 h. The volatiles are removed in vacuo, and the crude product is taken up in a minimum amount of pentane and subjected to column chromatography (silanized silica gel, 40 cm, ∅ 3 cm). The first orange zone contains unreacted 1· (18%). The second, brown zone is eluted with pentane to yield (Me$_2$P-η^6-C$_6$H$_5$)(η^6-C$_6$H$_6$)-V (12·, 0.56 g, 32%) as copper-colored platelets, mp 71−72 °C. From the third, brown zone, which is eluted with toluene, (Me$_2$P-η^6-C$_6$H$_5$)$_2$V (4·, 0.69 g, 32%) is obtained as dark brown prisms, mp 70−71 °C. Anal. Calcd for C$_{14}$H$_{17}$PV (267.21): C, 62.93; H, 6.41. Found: C, 62.42; H, 6.56. Calcd for C$_{16}$H$_{22}$P$_2$V (327.23): C, 58.72; H, 6.78. Found: C, 58.02; H, 6.86.

Use of tetramethyldiphosphane instead of dimethylchlorophosphane affords the same product distribution.

{(Me$_2$P-η^6-C$_6$H$_5$)$_2$V}$_2$Ni (7··). To a solution of bis(cyclooctadiene)nickel (6, 0.27 g, 1.0 mmol) in toluene (10 mL) is added at room temperature (Me$_2$P-η^6-C$_6$H$_5$)$_2$V (4·, 0.71 g, 2.2 mmol), dissolved in 20 mL of toluene; the mixture is stirred for 16 h. After filtration the brown solution is reduced to a volume of 5 mL, layered with 20 mL of pentane, and cooled to −20 °C. Crystallization affords 7·· (0.45 g, 60%) as small brown prisms, dec 262−263 °C. Anal. Calcd for C$_{32}$H$_{44}$NiP$_4$V$_2$ (713.17): C, 53.89; H, 6.22. Found: C, 53.92; H, 6.30.

{(Me$_2$P-η^6-C$_6$H$_5$)$_2$V}$_2$CoH (10··). A solution of (η^3-C$_8$H$_{13}$)-(η^4-C$_8$H$_{12}$)Co (9, 0.20 g, 0.72 mmol) and (Me$_2$P-η^6-C$_6$H$_5$)$_2$V (4·, 0.50 g, 1.5 mmol) in 30 mL of toluene is stirred for 3 h at −20 °C. The solvent is removed in vacuo, and the residue is extracted with three 30 mL portions of petroleum ether. The remaining solid is dissolved in a minimal amount of toluene and layered with low-boiling petroleum ether. Precipitation at 4 °C generates 10·· (0.23 g, 45%) as a microcrystalline brown material. Anal. Calcd for C$_{32}$H$_{45}$CoV$_2$P$_4$ (714.42): C, 53.80; H, 6.35. Found: C, 53.72; H, 6.47.

{(Me$_2$P-η^6-C$_6$H$_5$)$_2$Cr}$_2$CoH (11). This trinuclear complex was prepared as described for 10·· from 9 (0.22 g, 0.79 mmol) and (Me$_2$P-η^6-C$_6$H$_5$)$_2$Cr (5, 0.59 g, 1.8 mmol). In this case, the product 11 (0.31 g, 55%) could be obtained as red crystals of rhomboid shape. Anal. Calcd for C$_{32}$H$_{45}$CoCr$_2$P$_4$ (716.58): C, 53.63; H, 6.34. Found: C, 53.43; H, 6.23. ¹H NMR (D$_8$-THF, 300.13 MHz, 298 K): δ −12.92 (quint., 1 H, Co-H, $^2J_{CoH}$ = 32 Hz), 4.22 (m, 8 H, 2,6-H), 4.90 (m, 8 H, 3,5-H), 4.22 (m, 4 H, 4-H), 1.56 (s, 24 H, CH$_3$). ¹H NMR (D$_8$-THF, 300.13 MHz, 197 K): δ −16.35 (quint., 1 H, Co-H, $^2J_{CoH}$ = 29 Hz), 4.32 (m, 8 H, 2,6-H), 5.00 (m, 8 H, 3,5-H), 4.33 (m, 4 H, 4-H), 1.62 (s, 24 H, CH$_3$). ¹³C{¹H} NMR (D$_8$-THF, 75.47 MHz, 298 K): δ 102.4 (1-C), 78.7 (2,6-C), 75.4 (3,5-C), 75.0 (4-C), 27.0 (CH$_3$). ³¹P{¹H} NMR (D$_8$-THF, 116.7 MHz): 11.82 (297 K), 12.51 (183 K).

{(Me$_2$P-η^6-C$_6$H$_5$)(η^6-C$_6$H$_6$)V}$_2$Ni(CO)$_2$ (14··). (Me$_2$P-η^6-C$_6$H$_5$)(η^6-C$_6$H$_6$)V (12·, 0.134 g, 0.5 mmol) is dissolved in 20 mL of toluene, Ni(CO)$_4$ (32 μL, 0.25 mmol) is added, and the mixture is stirred for 12 h at room temperature. The reddish

(18) Fischer, E. O.; Reckziegel, A. *Chem. Ber.* **1961**, *94*, 2204.

(19) Otsuka, S.; Rossi, M. *J. Chem. Soc. (A)* **1968**, 2630.

(20) (a) Fischer, E. O.; Reckziegel, A. *Chem. Ber.* **1961**, *94*, 2204. (b) Fischer, E. O.; Hafner, W. *Z. Naturforsch.* **1955**, *10b*, 665.

(21) Sheldrick, G. M. *SHELXS-86*; University of Göttingen: Göttingen, Germany, 1986.

(22) Sheldrick, G. M. *SHELXL-93*; University of Göttingen: Göttingen, Germany, 1993.

(23) Sheldrick, G. M. *SHELXL-97*; University of Göttingen: Göttingen, Germany, 1997.

(24) Spek, A. L. *PLATON-94*, University of Utrecht: Utrecht, The Netherlands, 1994.

(25) *International Tables for Crystallography,* Vol. A, 2nd ed.; Kluwer Academic Publishers: Dordrecht, The Netherlands, 1989.

brown solution is filtered over a 2 cm layer of silanized silica gel, and the volume is reduced in vacuo to 5 mL. Layering with hexane leads to precipitation of **14··** (130 mg, 80%) as a black microcrystalline product. Anal. Calcd for $C_{30}H_{34}P_2O_2V_2$-Ni (649.12): C, 55.51; H, 5.27. Found: C, 54.92; H, 5.16. IR (toluene): ν_{CO} = 1988, 1924 cm^{-1}.

{(**Me₂P-η^6-C₆H₅)(η^6-C₆H₆)Cr}₂Ni(CO)₂ (15).** The preparation and product yield of **15** were identical to that of **14··**. However, crystallization afforded black crystals of **15**, which were suitable for X-ray diffraction. Anal. Calcd for $C_{30}H_{34}P_2O_2$-Cr₂ Ni (651.26): C, 55.32; H, 5.26. Found: C, 55.18; H, 5.23. IR (toluene): ν_{CO} = 1984, 1932 cm^{-1}. ^{1}H NMR (C₆D₆, 300.13 MHz, 298 K): δ 4.71 (m, 4 H, 2,6-H), 426 (m, 4 H, 3,5-H), 4.21 (m, 2 H, 4-H), 4.37 (s, 12 H, C₆H_6), 1.30 (d, 12 H, CH_3, $^3J_{PH}$ =

4.9 Hz). ^{13}C{^{1}H}NMR (C₆D₆, 75.47 MHz, 298 K): δ 77.1 (2,6-C), 74.4 (3,5-C), 73.6 (4-C), 76.4 (C₆H₆), 20.8 (CH₃), 202 (CO). ^{31}P NMR (C₆D₆, 116.7 MHz, 298 K): δ 4.6 (s).

Supporting Information Available: Tables of atomic coordinates, isotropic and anisotropic displacement parameters, and all bond lengths and angles. This material is available free of charge via the Internet at http://pubs.acs.org.

OM058027K